Available online at www.sciencedirect.com
ScienceDirect
Chemical Physics Letters 450 (2008) 178–185
CHEMICAL PHYSICS LETTERS
www.elsevier.com/locate/cplett

A reinvestigation of the gas phase reaction of boron atoms, $^{11}B(^2P_j)/^{10}B(^2P_j)$ with acetylene, $C_2H_2(X^1\Sigma_g^+)$

Fangtong Zhang [a,*], Xibin Gu [a], Ralf I. Kaiser [a,*], Holger Bettinger [b,*]

[a] Department of Chemistry, University of Hawai'i, Honolulu, HI 96822, USA
[b] Lehrstuhl für Organische Chemie II, Ruhr-Universität Bochum, 44780 Bochum, Germany

Received 12 August 2007; in final form 18 October 2007
Available online 25 October 2007

Abstract

The reaction dynamics of ground state boron atoms, $B(^2P_j)$, with acetylene, was reinvestigated and combined with novel electronic structure calculations. Our study suggests that the boron atom adds to the carbon–carbon triple bond of the acetylene molecule to yield initially a cyclic intermediate undergoing two successive hydrogen atom migrations to form ultimately an intermediate **i3**. The latter was found to decompose predominantly to the c-$BC_2H(X^2A')$ isomer plus atomic hydrogen via a tight exit transition state. To a minor amount, an isomerization of **i3**–**i4** prior to a hydrogen atom ejection forming the linear structure, $HBCC(X^1\Sigma^+)$, has to be taken into account. Since the c-$BC_2H(X^2A')$ and $HBCC(X^1\Sigma^+)$ isomers are separated by an isomerization barrier to ring closure of only 3 kJ mol^{-1}, internally excited $HBCC(X^1\Sigma^+)$ products can isomerize to the c-$BC_2H(X^2A')$ structure and vice versa.

1. Introduction

In recent years, boron–carbon clusters and their partially hydrogenated counterparts have received considerable attention both theoretically [1] and experimentally [2–7]. This is due to their importance in semi conductor processes [8,9] and as additives to rocket-propellants [10]. In chemical vapor deposition (CVD) processes involving diborane, hydrogen, and simple hydrocarbons like methane, boron often prevails as a transient reactant [11]; from the industrial viewpoint, these processes are important to manufacture boron-doped diamond films (p-type semiconductors, unconventional superconductor, UV Schottky photodiodes) and boron-doped hydrogenated amorphous carbon films via surface-wave mode microwave plasma CVD and their potential applications to photovoltaic cells [12]. Since atomic boron, $B(^2P_j)$, is isoelectronic with singly ionized carbon atoms, an understanding of elementary boron atom reactions can also assist to understand the chemistry in weakly ionized hydrocarbon plasmas. Here, $C^+(^2P_j)$ presents in important reactant and can contribute, for instance, to the formation of polycyclic aromatic hydrocarbons (PAHs) and their cationic counterparts [13].

In this context, it is important to note that an investigation of the reaction of ground state boron atoms, ^{11}B and ^{10}B, with acetylene has attracted substantial interest. These reactions access experimentally the BC_2H_2, BC_2H, and BC_2 potential energy surfaces (PES) of some of the smallest (hydrogenated) boron–carbon clusters. Small clusters like BC, BC_2 and B_2C were first observed in the early 1960s via mass spectrometry in the vapor phase over solid boron carbide heated to about 2300 K [14]. Later on, these molecules were successfully trapped in solid argon or neon matrices and characterized by electron spin resonance spectroscopy (ESR) [2]. The results suggested the at least one BC_2 isomer had a linear $BCC(X^2\Sigma^+)$ structure. As technology advanced, in 1990s, Martin et al. reinvestigated this system utilizing pulse laser ablation of boron–carbon pellets coupled with matrix isolation spectroscopy [15]. This study concluded that BC_2 was a cyclic molecule with a strong, symmetric BC_2 stretching frequency near 1200 cm^{-1}. Knight et al. confirmed that the ground state

* Corresponding authors. Fax: +1 808 956 5908.
E-mail addresses: fangtong@hawaii.edu (F. Zhang), ralfk@hawaii.edu (R.I. Kaiser), Holger.Bettinger@ruhr-uni-bochum.de (H. Bettinger).

0009-2614/$ - see front matter © 2007 Elsevier B.V. All rights reserved.
doi:10.1016/j.cplett.2007.10.067

of BC_2 in neon, argon, and krypton matrices is in fact the nonlinear symmetric structure with an X^2A_1 electronic ground state,[4] about 26 kJ mol^{-1} below the linear BCC($X^2\Sigma^+$) isomer [5].

The local minima of the BC_2H potential energy surface were studied first via low temperature spectroscopy via reaction of laser ablated boron atoms with acetylene molecules [16]. Besides the BC_2H_2 adducts, Andrews et al. identified two linear BC_2H isomers, i.e. HCCB($X^1\Sigma^+$) and HBCC ($X^1\Sigma^+$). However, the reaction mechanisms to form these structures could not be resolved explicitly. In 2001, Balucani et al. carried out the gas phase reaction of ground state boron atoms, B (^2P_j), with acetylene (C_2H_2($X^1\Sigma_g^+$)) utilizing the crossed molecular beams approach [17]. In this preliminary study, the authors found that the atomic boron versus atomic hydrogen exchange channel was open. The reaction dynamics were suggested to be indirect, proceed via addition of the boron atom to the carbon–carbon triple bond and form – after successive isomerization – the linear HBCC($X^1\Sigma^+$) isomer. In a complementary study, Geppert et al. [18] investigated in both kinetic and dynamic experiments the reaction of boron atoms with acetylene and D_2-acetylene. The authors indicated that both sets of results were best described by the presence of a very weak barrier in the entrance channel of the PES (0.18 kJ mol^{-1}). However, this investigation could not shed light on the nature of the BC_2H isomer(s) formed.

However, various aspects of this reaction have remained unanswered so far. First, due to the enhanced sensitivity and hence increasing signal-to-noise of the present crossed molecular beam experimental setup, we intent to investigate if only the atomic hydrogen or also the molecular hydrogen elimination channel is open. Secondly, we attempt to extract to what extent a hitherto neglected cyclic BC_2H isomer is involved in the chemical dynamics; recall that in the related reaction of ground state boron atoms with acetylene, both the linear and cyclic C_3H isomers were synthesized [17,19]. This study is combined with new, high level electronic structure calculations which can provide reaction energies within chemical accuracy (±5 kJ mol^{-1}). This will also allow us to reinvestigate the experimentally obtained reaction energy to form BC_2H isomer(s) within much lower error bars than studied previously to be compared with the new theoretical data.

2. Experimental setup, data analysis, and theoretical methods

The elementary reaction of ground state boron atoms, B(^2P_j), with acetylene, C_2 H_2($X^1\Sigma_g^+$) was studied in a universal crossed molecular beams machine under the single collision conditions. Briefly, a pulsed boron atom beam was generated in the primary source chamber by laser ablation of a boron rod at 266 nm (30 Hz) and seeded in neat helium carrier gas (99.9999%, Airgas; 4 atm) released by a Proch–Trickl pulsed valve. As monitored by the mass spectrometric detector, the ablation beam contains both ^{11}B and ^{10}B species in their nature abundances. After passing a skimmer, a four-slot chopper wheel selected a part out of the boron beam at a peak velocity v_p of 2070 ± 10 m s^{-1}; a speed ratio of 3.5 ± 0.2 was obtained. This part crossed a pulsed acetylene beam (99.99% after removal of acetone via zeolite traps and acetone-dry ice bath; 550 torr) released by a second pulsed valve perpendicularly in the interaction region. The segment of the acetylene beam was characterized by a peak velocity of 950 ± 20 m s^{-1} and a speed ratio of S = 16.0 ± 1.0. For the $^{11}B/C_2H_2$ and $^{10}B/C_2H_2$ systems, collision energies of 20.1 ± 0.2 kJ mol^{-1} and 18.7 ± 0.2 kJ mol^{-1}, respectively, were obtained. The reactively scattered species were monitored using a quadrupole mass spectrometric detector in the time-of-flight (TOF) mode after electron-impact ionization of the molecules at 90 eV. This detector could be rotated within the plane defined by the primary and the secondary reactant beams to allow taking angular resolved TOF spectra at specific mass-to-charge (m/z) ratios. At each angle,

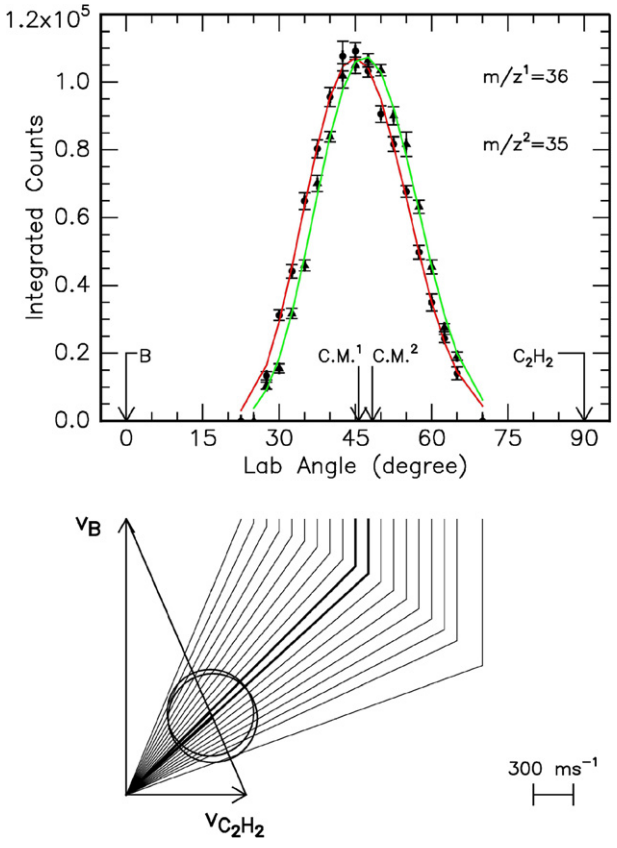

Fig. 1. Lower: Newton diagram for the $^{11}B/C_2H_2$ and $^{10}B/C_2H_2$ systems investigated. The circles show the maximum center-of-mass recoil velocity of the cyclic $^{11}BC_2H/^{10}BC_2H$ isomers assuming that no energy channels into the internal degrees of freedom. Upper: Laboratory angular distribution of the $^{11}BC_2H/^{10}BC_2H$ products at $m/z = 36$ (red) and 35 (green) respectively. Circles/triangles and 1σ error bars indicate experimental data, the solid red/green lines indicate the calculated distribution. The center-of-mass angles are indicated by C.M. The solid lines originating in the Newton diagram point to distinct laboratory angles whose times-of-flight are shown in Fig. 2. (For interpretation of the references to colour in this figure legend, the reader is referred to the web version of this article).

TOF spectra were accumulated up to 300 000 times to achieve a good signal-to-noise ratio. The recorded TOF spectra were then integrated and normalized to obtain a product angular distribution in the laboratory frame (LAB). Information on the chemical dynamics were gathered by fitting the TOF spectra and the LAB distributions using a forward-convolution routine [20,21]. Best fits of the TOF and laboratory angular distributions were achieved by refining the adjustable $T(\theta)$ and $P(E_T)$ parameters averaging over the apparatus functions and beam parameters.

Coupled cluster theory with single and double excitations (CCSD) was used for analytic gradient geometry optimization and computations of harmonic vibrational frequencies and zero-point energies by finite differences of analytic gradients in conjunction with Dunning's polarized double-ζ basis set (DZP) with one set of polarization functions on heavy atoms ($\alpha_C = 0.75$, $\alpha_B = 0.70$) and on hydrogen ($\alpha_H = 1.00$) [22,23]. The CCSD(T) method, which includes the perturbative treatment of triple excitations, was used for single-point energy computations in conjunction with Dunning's [24] correlation consistent cc-pVXZ (X = T, Q) basis sets as well as for the geometry optimization of selected species with the DZP basis set. In order to arrive at highly reliable reaction energies, W1 theory [25] modified to use spin-unrestricted coupled cluster theory was employed along with completely renormalized CR-CCSD(T) [26]. The computations employed a spin-unrestricted reference function for radical species and were performed with the GAUSSIAN 03 [27] or Gamess [28] programs.

3. Results

To investigate the atomic hydrogen and potential molecular hydrogen loss pathways, reactive scattering signal was recorded at mass-to-charge ratios, m/z, of 36 and 35. Here, signal at $m/z = 36$ could originate from the ^{11}B versus atomic hydrogen pathways and the inherent formation of $^{11}BC_2H$. In principle, ion counts at $m/z = 35$ could have up to three contributions: (i) the ionized $^{11}BC_2^+$ reaction

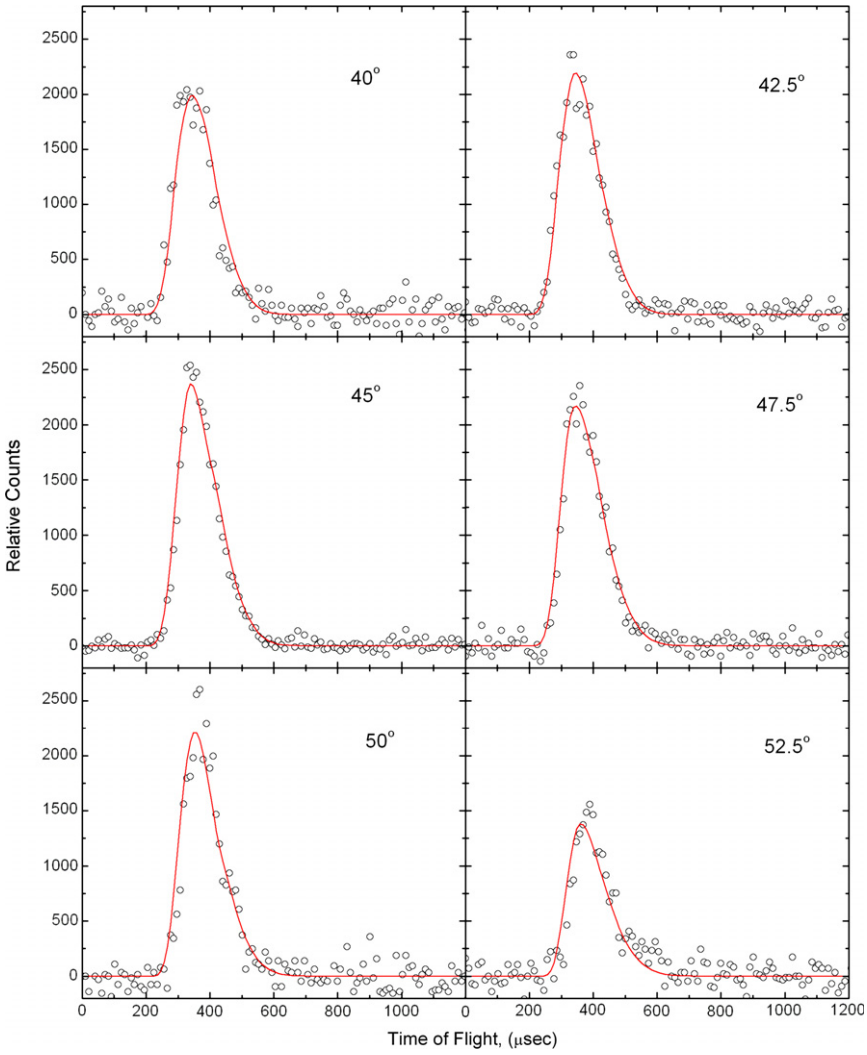

Fig. 2a. Time-of-flight data at $m/z = 36$ for the indicated laboratory angles. The circles represent the experimental data, and the solid line represents the fit.

product formed in the ^{11}B versus molecular hydrogen loss pathway, (ii) $^{11}BC_2^+$ formed in dissociative ionization of the $^{11}BC_2H$ reaction product, and (iii) the ionized $^{10}BC_2H$ product synthesized in the ^{11}B versus atomic hydrogen exchange channel. As a matter of fact, the TOF spectra recorded at $m/z = 36$ and 35 as well as the extracted LAB distributions at these mass-to-charge ratios were found to be different and *not* superimposable (Figs. 1 and 2). Both LAB distributions have a similar shape and extend only 35° within the scattering plane. This suggests that the averaged translational energy released in the translational degrees of freedom of the reaction products was relatively small. The LAB distributions extracted from the TOF spectra at $m/z = 36$ and 35 peak at 45.0° and 47.5° close to the corresponding center-of-mass angles of $47.3 \pm 0.7°$ and $50.0 \pm 0.6°$, for the $^{11}B/C_2H_2$ and $^{10}B/C_2H_2$ systems, respectively. Due to the lower intensity of the atomic boron beam, less signal of the reactively scattered products, lower signal-to-noise ratios of the TOF spectra, and hence larger error bars in the LAB distributions, a previous study could not resolve the differences in the TOF and LAB distributions of data recorded at $m/z = 36$ and 35 [17,19].

To shed light on the open reaction channels, a forward-convolution routine was utilized to fit the laboratory data at $m/z = 36$ and 35. At $m/z = 36$, a single channel could fit the experimental data (Fig. 3). This suggests that in agreement with an earlier study, the ^{11}B versus hydrogen replacement pathway and the formation of $^{11}BC_2H$ isomer(s) is open. Here, the corresponding center-of-mass translational energy distribution was found to peak well away from zero translational energy at about 10–20 kJ mol^{-1}. Likewise, this distribution extends to a maximum translational energy of 48 ± 4 kJ mol^{-1}. Recall that the latter represents the sum of the reaction exoergicity plus the collision energy for those reaction products without rovibrational excitation. Therefore, by subtracting

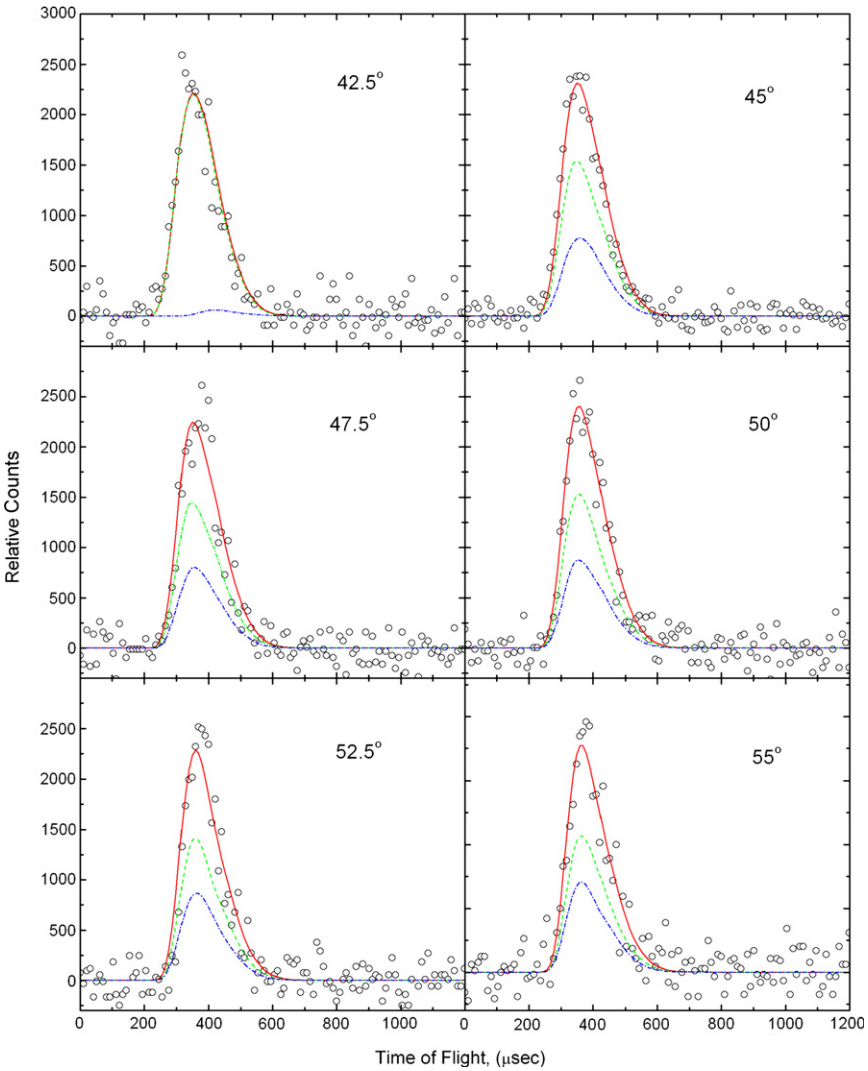

Fig. 2b. Time-of-flight data at $m/z = 35$ for the indicated laboratory angles. The circles represent the experimental data, and the solid line represents the fit (blue line: $^{10}BC_2H^+$; green line $^{11}BC_2^+$; red: both contributions). (For interpretation of the references to colour in this figure legend, the reader is referred to the web version of this article.)

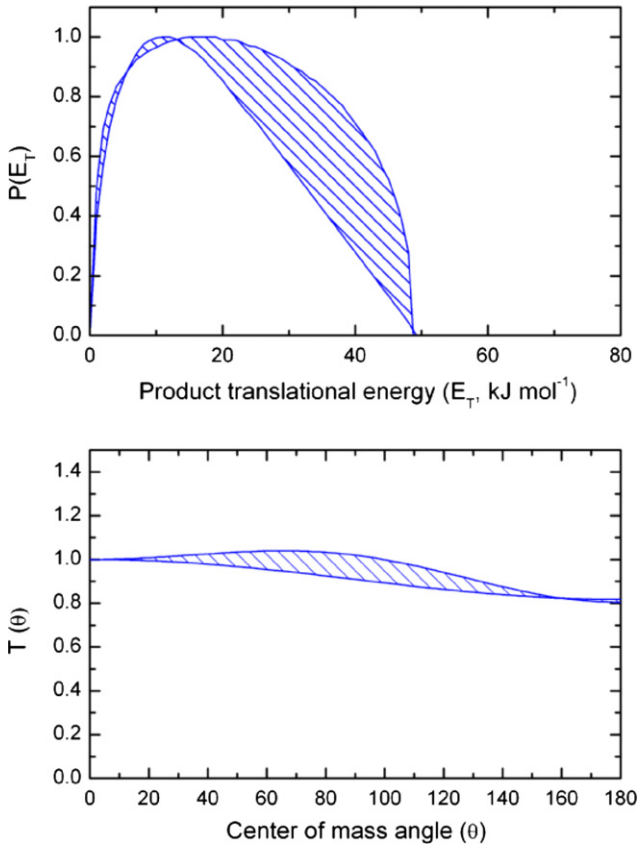

Fig. 3. Upper: Center-of-mass translational energy flux distribution for the reaction $^{11}B(^2P_j) + C_2H_2(X^1\Sigma_g^+)$. The two lines limit the range of acceptable fits to within 1σ error bars. Lower: Center-of-mass angular flux distribution for the reaction $^{11}B(^2P_j) + C_2H_2(X^1\Sigma_g^+)$. The two lines limit the range of acceptable fits to within 1σ error bars.

the collision energy (20.1 ± 0.2 kJ mol^{-1}) from the latter, the reaction is found to be exoergic 28 ± 4 kJ mol^{-1}. This data as the same order of magnitude than previously study (31 ± 10 kJ mol^{-1}), but holds lower error bars due to the enhanced sensitivity of the setup. Also, the $T(\theta)$ is slightly forward scattered with respect to the ^{11}B beam and extends over the complete angular range from 0° to 180°. This confirms the indirect nature of the reaction pathway leading to the formation of $^{11}BC_2H$ isomer(s).

At $m/z = 35$, the situation is more complicated, and two channels had to be utilized to fit the LAB and TOF data. Recall that the LAB and TOF spectra at $m/z = 36$ and 35 were found to be *not* superimposable. The first channel accounts for $^{11}BC_2^+$ which is formed via dissociative ionization of the $^{11}BC_2H$ reaction product. The second channel had to utilize the mass combination of ^{10}B with acetylene ($m/z = 26$) and the product mass of $m/z = 35$, i.e. ionized $^{10}BC_2H$. The center-of-mass functions of these pathways are essentially identical to those depicted in Fig. 3. A combination of these channels could fit both the TOF spectra and the LAB distributions simultaneously. It was not necessary to include the molecular hydrogen elimination pathway in the fitting routing. Therefore, we can conclude that the non-similarity of the TOF and LAB distributions at $m/z = 36$ and 35 is solely the effect of the distinct center-of-mass angles of the $^{11}B/C_2H_2$ and $^{10}B/C_2H_2$ systems, but certainly not of an involvement of a molecular hydrogen elimination channel.

A reinvestigation of the $^{11}BC_2H_2$ potential energy surface and comparison with a previous theoretical study [17] suggests similar energetics of the $^{11}BC_2H_2$ intermediates (Fig. 4). The newly computed energies based on the (U)CCSD/DZP geometries are systematically lower by 2–5 kJ mol^{-1}. However, also various differences exist. First, in the entrance channel our present study was unable to find a transition state connecting the reactants with intermediate **i6**. On the other hand, we could locate a weakly bound van-der-Waals complex and a transition state for the addition of boron to the carbon–carbon triple bond forming **i1**. These two stationary points ($^2B_2$ electronic states) are essentially isoenergetic and are 12 kJ mol^{-1} below reactants in energy. Both stationary points disappear when using larger basis sets for geometry optimization, and hence are not depicted in Fig. 4. The experiments by Geppert et al. indicate a small barrier of 0.18 kJ mol^{-1} in the entrance channel, [18] but our computations do not indicate the existence of a potential energy entrance barrier. In addition, we found two additional intermediates **i7** and **i8**. All attempts to locate a HCBCH intermediate similar to propargylene (HCCCH) on the ground state surface failed. Most important, our present computations show that a novel cyclic isomer, c-HBC$_2$(X^2A'), is the most stable HBC_2 entity (Fig. 5). While the symmetric c-HBC$_2$(X^2A') isomer is a saddle point, distortion to a strongly asymmetric structure with a CCB angle of 86.2° results upon relaxing symmetry constraints from C_{2v} to C_s. This isomer was not observed previously as it is nonexistent on the B3LYP PES, but it exists at CCSD(T)/DZP level. At our highest level of theory, CR-CCSD(T)/cc-pVQZ//CCSD(T)/DZP, it is about 5 kJ mol^{-1} lower in energy than the corresponding HBCC ($X^1\Sigma^+$) structure. The cyclic c-BC_2 molecule can be formed via a tight exit transition state from the cyclic intermediate **i3** via hydrogen atom emission. The stability of **i3** can be understood in light of its aromatic character. This intermediate can be derived from the aromatic borirene molecule by abstracting a hydrogen atom from the carbon atom. The resulting radical **i3** is still aromatic; the unpaired electron is in the molecular plane of **i3**, similar to the carbon radical center in the phenyl radical. Both c-HBC$_2$(X^2A') and HBCC($X^1\Sigma^+$) can isomerize via a barrier located only 3 kJ mol^{-1} above the linear structure and hence 6 kJ mol^{-1} below the energy of the separated atomic boron and acetylene reactants. It should be stressed that a fourth possible C_2BH isomer was located, too. However the formation of the HCBC($X^1\Sigma^+$) plus atomic hydrogen is endoergic by 240 kJ mol^{-1} and hence energetically not accessible under our experimental conditions. Based on these considerations, only the HBCC + H and the c-C_2BH channels are energetically accessible, whereas the

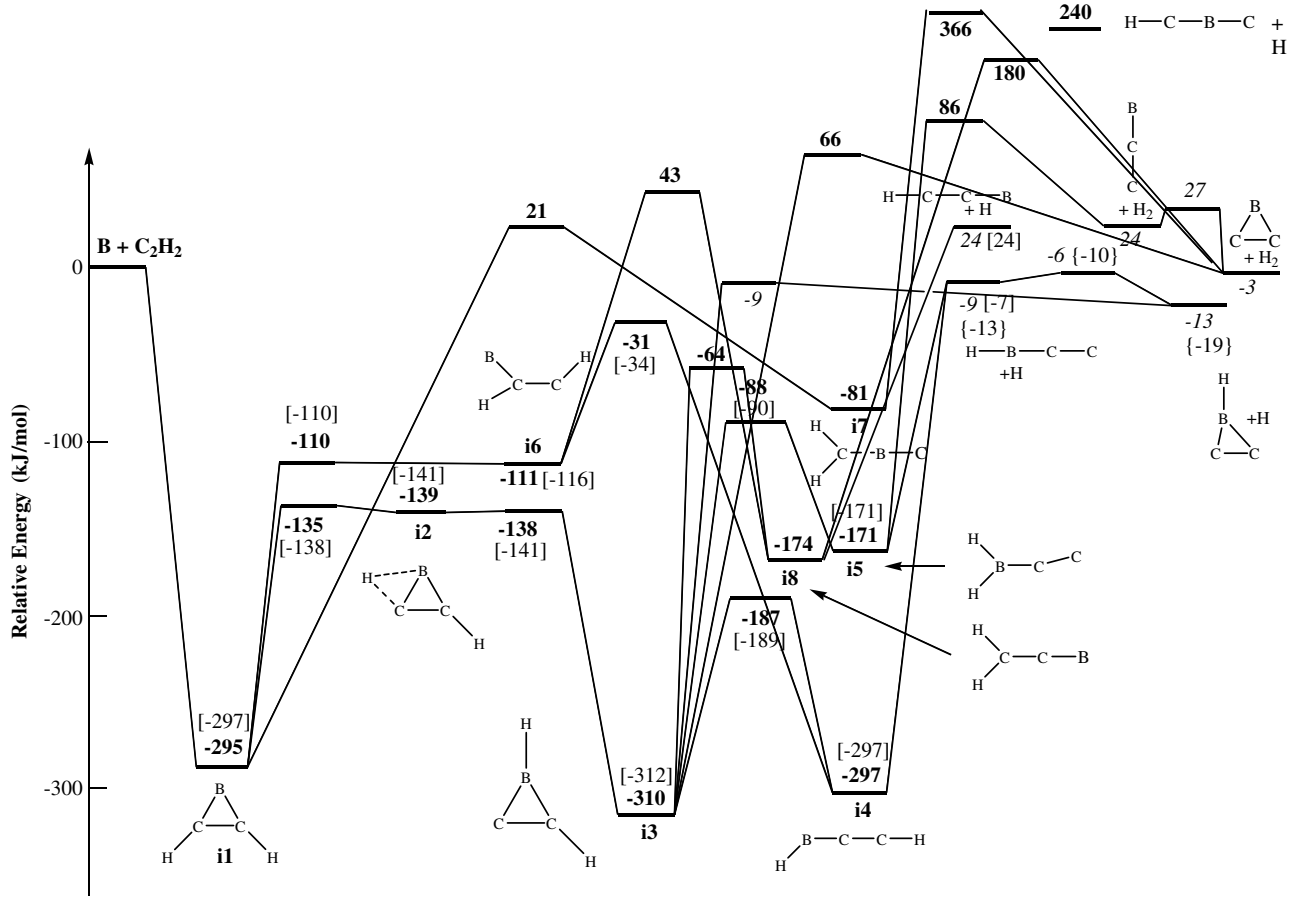

Fig. 4. Potential energy surface of the reaction of ground state boron atoms, $^{11}B(^2P_j)$, with acetylene. Bold type: CCSD(T)/cc-pVTZ//CCSD/DZP + ZPVE(CCSD/DZP); italics: CCSD(T)/cc-pVQZ//CCSD(T)/DZP + ZPVE(CCSD/DZP). Data in curly brackets are based on the W1 model and on CR-CCSD(T)//cc-pVQZ//CCSD(T)/DZP + ZPVE(CCSD/DZP), see text. The data in square brackets are taken from Ref. [17].

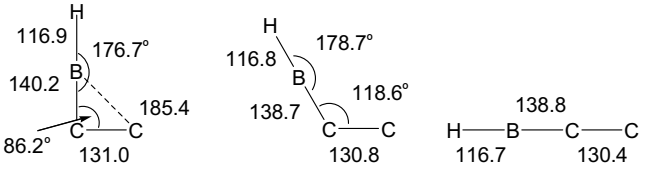

Fig. 5. Structures of the c-$BC_2H(X^2A')$ (left) and $HBCC(X^1\Sigma^+)$ (right) isomers together with the transition state (center) connecting both structures as computed at the CCSD(T)/DZP level of theory. Angles are given in degrees, bond lengths in picometers.

HCCB + H, HCBC + H, BCC + H_2, and c-C_2B + H_2 pathways are closed (Fig. 4).

The distortion away from C_{2v} symmetry can be considered a second-order Jahn–Teller distortion (SOJT). The LUMO (b_2 symmetry) is very low in energy, and thus a small energy separation between HOMO (a_1 symmetry) and LUMO results. The distortion away from C_{2v} is also of b_2 symmetry, thus the $a_1 \times b_2 \times b_2$ direct product contains the a_1 irreducible representation, and the SOJT is symmetry allowed. On the other hand, the open-shell singlet resulting from a different occupation of the frontier orbitals ($^1B_2$) is the lowest energy excited state of c-HBC_2. It is 2.91 eV (full valence CAS/6-31G*) higher in energy than the ground state. According to analytic second derivative computations at the full valence CAS level, the $^1A_1$ state is a first-order saddle point, while the excited $^1B_1$ state is a minimum.

4. Discussion

Based on these considerations, we can compare now the computations with the experimental data. First, the experimentally derived reaction energy of -28 ± 4 kJ mol^{-1} has to be compared with the computed reaction energies. Based on W1 theory, we obtain an energy of -13.4 kJ mol^{-1} for formation of the $HBCC(X^1\Sigma^+)$ isomer plus atomic hydrogen. As W1 theory is based on B3LYP geometries, we could not compute the c-$BC_2H(X^2A')$ isomer; but taking into account the 5.3 kJ mol^{-1} preference of the latter obtained at the CR-CCSD(T) level as discussed above, we arrive at an energy of -19 ± 5 kJ mol^{-1} for formation of the c-$BC_2H(X^2A')$ isomer plus atomic hydrogen. Therefore, we can conclude that within the error limits, at least the c-$BC_2H(X^2A')$ isomer is formed. Also, we have to recall that the $P(E_T)$ depicted a distribution maximum in the range of 10–20 kJ mol^{-1}. In the most favorable case, this is indicative of a tight exit transition state and hence the

existence of an exit barrier [29]. Therefore, a closer look at the pertinent PES suggests that the cyclic intermediate **i3** decomposes via a tight exit transition state located about 10 kJ mol^{-1} above the c-$BC_2H(X^2A')$ plus hydrogen atom products. On the other hand, both intermediates **i4** and **i5** fragment without exit barrier to the linear isomer, $HBCC(X^1\Sigma^+)$, and a hydrogen atom. If this reaction follows statistical patters, i.e. a complete energy randomization prior to the decomposition of the decomposing complex(es), we expect that the boron atom adds to the carbon–carbon triple bond forming intermediate **i1**. The latter isomerizes via two successive hydrogen shifts to yield ultimately the cyclic structure **i3**. This intermediate could decompose to yield the c-$BC_2H(X^2A')$ isomer plus atomic hydrogen via a tight exit transitions state. Based on the PES, we also expect that **i3** isomerizes to a minor amount to **i4** before this intermediate loses a hydrogen atom and forms $HBCC(X^1\Sigma^+)$. We would like to stress that the c-$BC_2H(X^2A')$ and $HBCC(X^1\Sigma^+)$ isomers formed are rovibrationally excited. Since the isomerization barrier between these structures is only 3 kJ mol^{-1} and below the energy of the separated reactants, a isomerization between the initially formed c-$BC_2H(X^2A')$ and $HBCC(X^1\Sigma^+)$ is expected (Fig. 5).

Considering potential molecular hydrogen loss pathways, the computations correlate nicely with the failed detection of any C_2B isomer. Although the formation of the c-$BC_2(X^2A')$ isomer plus molecular hydrogen is weakly exoergic, the transition state connecting **i3** and c-$BC_2(X^2A')$ is – similar to those connecting **i7** and **i8** with c-$BC_2(X^2A')$ – energetically not accessible under our experimental conditions. Also, all attempts to optimize a cyclic H_2CCB intermediate in which both hydrogen atoms are connected to a single carbon atom failed. Therefore, although c-$BC_2(X^2A')$ is energetically accessible, no low energy reaction pathways from any reaction intermediate exist. However, our calculations predict that the $BCC(X^2\Sigma^+)$ structure can isomerize via a small barrier of only 3 kJ mol^{-1} to c-$BC_2(X^2A')$. However, the initial synthesis of $BCC(X^2\Sigma^+)$ plus molecular hydrogen is endoergic by 24 kJ mol^{-1} and involves a tight exit transition state located 86 kJ mol^{-1} above the separated reactants. This is higher than our collision energy; consequently, this pathway is closed, too. Recall that a previous study suggested that the cyclic isomer is more stable by about 26 kJ mol^{-1} compared to the linear structure (5). Our calculations verify this difference and confirm that the cyclic molecule is lower in energy by 27 kJ mol^{-1} compared to the linear structure.

5. Conclusions

The reaction dynamics of ground state boron atoms, $B(^2P_j)$,with acetylene, was reinvestigated and combined with novel electronic structure calculations. By utilizing an intense atomic boron beam and highly sensitive detector setup, it was feasible to discriminate the laboratory angular distributions and the TOF spectra of the $^{11}B/C_2H_2$ system from the $^{10}B/C_2H_2$ reaction. Also, the theoretical investigations demonstrated for the first time the existence of a cyclic $BC_2H(X^2A')$ structure which could not be identified in a previous study. Our combined investigations suggest that the boron atom adds to the carbon–carbon triple bond of the acetylene molecule to yield a cyclic intermediate **i1** via indirect scattering dynamics. The latter undergoes two successive hydrogen atom migrations to form the cyclic intermediate **i3**. Based on the shape of the derived center-of-mass translational energy distribution, we inferred that **i3** decomposes to c-$BC_2H(X^2A')$ isomer plus atomic hydrogen via a tight exit transition state. We cannot exclude an isomerization of **i3**–**i4** prior to a hydrogen atom ejection forming also the linear structure, $HBCC(X^1\Sigma^+)$. Based on the height of the transition state separating **i3** and **i4**, this rearrangement is expected to be fast. Nevertheless, based on the high energy cutoff of the center-of-mass translational energy distribution, it is evident that the c-$BC_2H(X^2A')$ must be synthesized; a sole formation of $HBCC(X^1\Sigma^+)$ cannot account for the experimental data. Also, both the c-$BC_2H(X^2A')$ and $HBCC(X^1\Sigma^+)$ isomers are separated by an isomerization barrier to ring closure of only 3 kJ mol^{-1} with respect to $HBCC(X^1\Sigma^+)$. Therefore, if the internally excited $HBCC(X^1\Sigma^+)$ is formed initially, it can rearrange to the c-$BC_2H(X^2A')$ structure and vice versa. Finally, our study confirms the absence of a molecular hydrogen pathway and the formation of any BC_2 molecules. These investigations should also trigger a study of the corresponding ionization potentials of the cyclic and linear c-$BC_2H(X^2A')$ and $HBCC(X^1\Sigma^+)$ isomers utilizing tunable vacuum ultraviolet radiation in a similar manner as conducted recently for the linear and cyclic C_3H isomers at the advanced light source [30].

Acknowledgements

This material is based upon work supported by the Air Force Office of Scientific Research (W911NF-05-1-0448). HFB acknowledges support from the Deutsche Forschungsgemeinschaft through a Heisenberg Fellowship.

References

[1] C.-G. Zhan, S. Iwata, J. Phys. Chem. A 101 (1997) 591.
[2] W.C. Easley, W. Weltner Jr., J. Chem. Phys. 52 (1970) 1489.
[3] J.D. Presilla-Marquez, C.W. Larson, P.G. Carrick, C.M.L. Rittby, J. Chem. Phys. 105 (1996) 3398.
[4] L.B. Knight Jr., S. Cobranchi, E. Earl, A.J. McKinley, J. Chem. Phys. 104 (1996) 4927.
[5] C. Leonard, G. Chambaud, P. Rosmus, S. Carter, N.C. Handy, M. Wyss, J.P. Maier, J. Chem. Phys. 113 (2000) 5228.
[6] M. Wyss, M. Grutter, J.P. Maier, J. Phys. Chem. A 102 (1998) 9106.
[7] T. Shirasaki, A. Derre, M. Menetrier, A. Tressaud, S. Flandrois, Carbon 38 (2000) 1461.
[8] A. Van Orden, R.J. Saykally, Chem. Rev. 98 (1998) 2313, Washington, DC.
[9] I. Caretti, I. Jimenez, R. Gago, D. Caceres, B. Abendroth, J.M. Albella, Diam. Relat. Mater. 13 (2004) 1532.

[10] J.M. Mota, J. Abenojar, M.A. Martinez, F. Velasco, A.J. Criado, J. Solid State Chem. 177 (2004) 619.
[11] T.T. Xu, A.W. Nicholls, R.S. Ruoff, Nano 1 (2006) 55.
[12] S.B. Wang, P.R. Zhu, K. Feng, Mater. Chem. Phys. 64 (2000) 10.
[13] A.M. Savel'ev, A.M. Starik, Tech. Phys. 51 (2006) 444.
[14] G. Verhaegen, F.E. Stafford, M. Ackerman, J. Drowart, Nature 193 (1962) 1280, London, United Kingdom.
[15] J.M.L. Martin, P.R. Taylor, J.T. Yustein, T.R. Burkholder, L. Andrews, J. Chem. Phys. 99 (1993) 12.
[16] L. Andrews, P. Hassanzadeh, J.M.L. Martin, P.R. Taylor, J. Phys. Chem. 97 (1993) 5839.
[17] N. Balucani, O. Asvany, Y.T. Lee, R.I. Kaiser, N. Galland, M.T. Rayez, Y. Hannachi, J. Comput. Chem. 22 (2001) 1359.
[18] W.D. Geppert, F. Goulay, C. Naulin, M. Costes, A. Canosa, S.D. Le Picard, B.R. Rowe, Phys. Chem. Chem. Phys. 6 (2004) 566.
[19] R.I. Kaiser, N. Balucani, N. Galland, F. Caralp, M.T. Rayez, Y. Hannachi, Phys. Chem. Chem. Phys. 6 (2004) 2205.
[20] M. Vernon, Ph. D., University of California, Berkley, CA, 1981.
[21] M.S. Weiss, Ph. D., University of California, Berkley, CA, 1986.
[22] T.H. Dunning, J. Chem. Phys. 53 (1970) 2823.
[23] EMSL-Citation-DZP. The DZP basis set was obtained from the Extensible Computational Chemistry Environment Basis Set Database, Version 02/02/06, as developed and distributed by the Molecular Science Computing Facility, Environmental and Molecular Sciences Laboratory which is part of the Pacific Northwest Laboratory, P.O. Box 999, Richland, Washington 99352, USA, and funded by the US Department of Energy. The Pacific Northwest Laboratory is a multi-program laboratory operated by Battelle Memorial Institute for the US Department of Energy under contract DE-AC06-76RLO 1830. Contact Karen Schuchardt for further information.
[24] T.H. Dunning, J. Chem. Phys. 90 (1989) 1007.
[25] J.M.L. Martin, G.d. Oliveira, J. Chem. Phys. 111 (1999) 1843.
[26] P. Piecuch, S.A. Kucharski, K. Kowalski, M. Musial, Comp. Phys. Commun. 149 (2002) 71.
[27] M.J. Frisch et al., GAUSSIAN 03, Revision B.4. Gaussian, Inc., Pittsburgh PA, 2003.
[28] M.W. Schmidt et al., J. Comput. Chem. 14 (1993) 1347.
[29] R.I. Kaiser, N. Balucani, Acc. Chem. Res. 34 (2001) 699.
[30] R.I. Kaiser, L. Belau, S.R. Leone, M. Ahmed, Y. Wang, B.J. Braams, J.M. Bowman, ChemPhysChem 8 (2007) 1236.